ACS OMEGA

http://pubs.acs.org/journal/acsodf

Article

Activation of H_2S by Atomic Cr, Mn, and Fe: Matrix Infrared Spectra and Quantum Chemical Calculations

Jie Zhao and Xuefeng Wang*

Cite This: *ACS Omega* 2022, 7, 29337−29343

Read Online

ACCESS | Metrics & More | Article Recommendations | Supporting Information

ABSTRACT: Hydrogen sulfide is toxic and corrosive gas abundantly available in nature. The activation of hydrogen sulfide to produce hydrogen and elemental sulfur is of great significance for possible applications in toxic pollutant control and hydrogen energy regeneration. The activation of H_2S by transition metal atoms (M = Cr, Mn, and Fe) has been studied by low-temperature matrix isolation infrared spectroscopy and quantum chemical calculations. Experimental and theoretical results indicate that the reaction between ground-state M atoms and H_2S is inhibited by the repulsive interactions between the reactants. After being excited upon photolysis, the corresponding excited-state M atoms react with H_2S molecules spontaneously. The produced insertion product HMSH further decomposed to metal sulfides upon full-arc mercury lamp irradiation by the splitting of hydrogen.

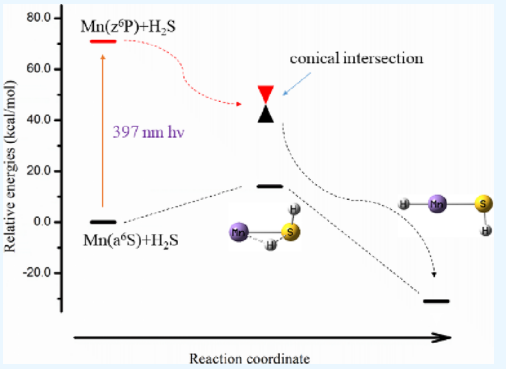

INTRODUCTION

Toxic hydrogen sulfide originates from nature, and industrial waste gases are responsible for the formation of aerosols and acid rain. The common process utilized to dispose hydrogen sulfide is the Claus process.[1] Meanwhile, the potential for hydrogen generation from hydrogen sulfide is lost in the Claus process. The splitting of hydrogen sulfide to produce hydrogen and sulfur is of great significance for toxic pollution control as well as hydrogen energy regeneration. Numerous materials such as metals, metal oxides, and metal sulfides have been explored as possible catalysts for hydrogen sulfide decomposition.[2−4] The low-temperature matrix isolation technique is useful in the reaction mechanism study. The activation of H_2S by laser-ablated group 4[5] and group 5[6] transition metal atoms in a low-temperature argon matrix takes place spontaneously, and the produced insertion products decompose to metal sulfides and hydrogen upon photoirradiation. Laser-ablated Th and U atoms react with H_2S on the annealing processes to produce H_2ThS and H_2US, respectively. The products further decompose to metal sulfides and hydrogen on broadband mercury lamp irradiation.[7]

For the purpose of obtaining more possible catalysts for the activation of H_2S, matrix isolation infrared spectroscopy and quantum calculations were employed to study the reaction mechanisms of transition metal atoms (M = Cr, Mn, and Fe) with hydrogen sulfide molecules in this work. We will show that laser-ablated Cr, Mn, and Fe atoms react with H_2S molecules in solid argon upon photolysis to produce the insertion product HMSH.

EXPERIMENTAL AND THEORETICAL METHODS

The experimental setup for laser ablation and matrix isolation infrared spectroscopy has been described in detail previously.[8,9] Briefly, a fundamental Nd:YAG laser (1064 nm, 10 Hz repetition rate with 10 ns pulse width) was focused on a rotating metal target. The laser-ablated Cr, Mn, or Fe metal atoms were co-deposited with hydrogen sulfide diluted in an argon matrix (typically 0.3%) on a 5 K CsI window for 1 h. After sample co-deposition, the Fourier transform infrared spectra were recorded between 400 and 4000 cm^{-1} at 0.5 cm^{-1} resolution using a Bruker 80 V spectrometer with a liquid nitrogen-cooled broadband MCT detector. Then, samples were annealed to the desired temperature and exposed to light with selected wavelengths to induce further reaction. A mercury lamp (75 W, without a globe) was used as a light source in the photolysis process with the aid of band filters to allow light of selected wavelength to pass through.

All the calculations were performed with the Gaussian 09 software package.[10] The def2-TZVPP basis sets were employed for all atoms. Structures of relative species were fully optimized, and harmonic frequencies were calculated analytically on the optimized structures. Transition states were characterized with one imaginary frequency and confirmed to

Received: June 8, 2022
Accepted: July 29, 2022
Published: August 10, 2022

https://doi.org/10.1021/acsomega.2c03594
ACS Omega 2022, 7, 29337−29343

link the corresponding products and reactants by intrinsic reaction coordinate calculations (IRC). Time-dependent density functional theory (TDDFT) at the B3LYP theoretical level was used to calculate the potential energy surfaces for the excited states.

RESULTS

Matrix isolation infrared spectroscopy was employed to study the reaction of laser-ablated transition metal atoms M (M = Cr, Mn, and Fe) with H_2S molecules diluted in the argon matrix (typically 0.3%). Besides the absorptions due to reactants and impurities such as water existing in all our experiments, absorptions due to chromium hydrides (CrH and CrH_2)[11] and chromium sulfides (CrS and CrS_2)[12] and two new absorptions at 1661.8 and 1683.4 cm^{-1} were identified in the experiments of Cr + H_2S in the solid argon matrix. Absorptions contributed from MnH, MnH_2,[13] and MnS[14] and a new absorption at 1661.6 cm^{-1} were identified in the experiments of Mn with H_2S by infrared spectroscopy. In the reaction of Fe + H_2S in the solid argon matrix, absorptions due to FeH_2,[15] FeS, and FeS_2[16] and two new absorptions at 1731.6 and 1688.9 cm^{-1} were identified. The assignments of the absorptions will be discussed in detail below.

HCrSH and $HCr(SH)_2$. The spectra in selected regions from reactions of laser-ablated Cr atoms with H_2S are presented in Figure 1 and Figure s1 in the Supporting Information.

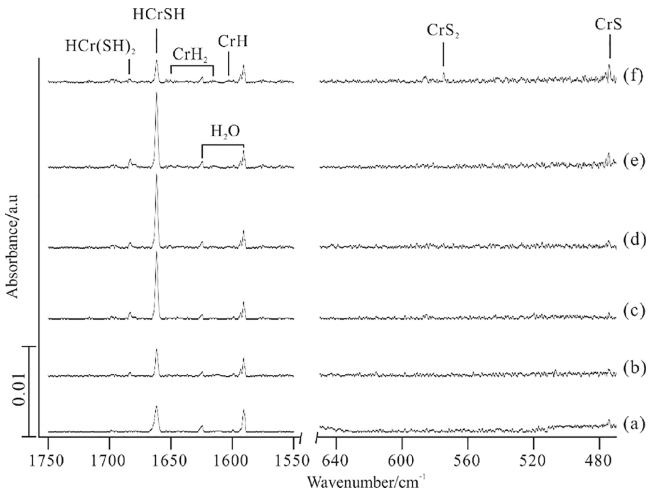

Figure 1. Spectra in selected regions from the reaction of Cr with 0.3% H_2S in the argon matrix: (a) 1 h co-deposition, (b) 25 K annealing, (c) 5 min >400 nm photolysis, (d) 5 min >270 nm photolysis, (e) 25 K annealing, and (f) 5 min full-arc mercury lamp irradiation.

Absorptions due to CrH (1603.3 cm^{-1}) and CrH_2 (1614.5 and 1650.9 cm^{-1}) were identified.[11] The absorption at 1661.8 cm^{-1} appeared after co-deposition and greatly enhanced upon >400 nm photolysis. In the reaction of Cr + 0.1% H_2S + 0.1% D_2S + 0.1% HDS in the solid argon matrix (Figure 2), the deuterium counterpart of 1661.8 cm^{-1} absorption appeared at 1198.8 cm^{-1}, giving an H/D isotopic ratio of 1.3862. The band position and H/D isotopic ratio are appropriate to the Cr−H stretching mode, indicating the existence of a Cr−H subunit in the complex. Compared with the Cr−H stretching absorption assigned to HCrOH[17] (1639 cm^{-1}), $HCrSiH_3$[18] (1645.7 cm^{-1}), and $HCrGeH_3$[19] (1656 cm^{-1}), the 1661.8 cm^{-1} absorption is suitable for the Cr(II)−H stretching vibration.

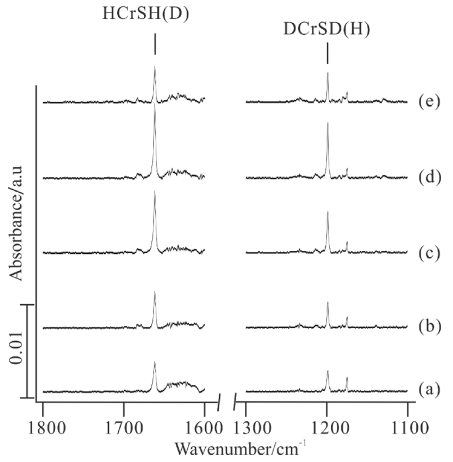

Figure 2. Spectra in selected regions from the reaction of Cr with 0.1% H_2S + 0.1% HDS + 0.1% D_2S in the argon matrix: (a) 1 h co-deposition, (b) 25 K annealing, (c) 5 min >400 nm photolysis, (d) 5 min >270 nm photolysis, and (e) 5 min full-arc mercury lamp irradiation.

Upon full-arc mercury lamp irradiation, absorption at 1661.8 cm^{-1} was nearly destroyed, accompanied by the appearance of absorption due to CrS (476.4 cm^{-1}),[12] indicating the conversion from the complex contributing to the 1661.8 cm^{-1} absorption to CrS upon photolysis. We assigned this absorption to HCrSH.

Absorption at 1683.4 cm^{-1} appeared as weak absorption after the annealing of the sample to 25 K and tripled upon the following >400 nm photolysis. The 1683.4 cm^{-1} absorption is 21.6 cm^{-1} higher than the Cr−H stretching mode of HCrSH. This absorption is suitable for the Cr−H stretching mode. No other absorption was observed to track with this absorption. It suggests the existence of a Cr−H subunit in the complex. Absorption at 1683.4 cm^{-1} was nearly destroyed, and absorption due to CrS_2[12] appeared upon full-arc mercury lamp irradiation, indicating the conversion of the complex to CrS_2. Accordingly, the 1683.4 cm^{-1} absorption is assigned to $HCr(SH)_2$.

Density functional theory calculations at the B3LYP theoretical level were carried out to further prove our assignments (Table 1). HCrSH was calculated to have a ^5A ground state with Cr−H stretching vibration predicted at 1708.2 cm^{-1} by harmonic frequency calculation (overestimated the experimental value by 2.8%). The predicted H/D isotopic ratio (1.3999) matches the experimental value (1.3862) well. The Cr−H stretching vibration of $HCr(SH)_2$ predicted at 1740.1 cm^{-1} by B3LYP calculations overestimates the experimental value (1683.4 cm^{-1}) by 3.4%. The predicted H/D isotopic ratio of 1.3994 is consistent with the experimental value of 1.3863.

HMnSH. Figure 3 presents the infrared spectra in selected regions from the reaction of laser-ablated Mn atoms with H_2S in solid argon. After annealing to 25 K, weak absorption at 1661.6 cm^{-1} sharpened and absorptions due to MnH_2 (1592.3 cm^{-1}) and MnH (1477.9 cm^{-1})[13] appeared. The 1661.6 cm^{-1} absorption enhanced by about 10% upon >350 nm irradiation and increased by about 10% again upon >300 nm photo-irradiation. After being exposed to full-arc mercury lamp irradiation, the absorption decreased by about 10% accompanied by the enhancement of absorption due to MnS[14] at 507.1 cm^{-1}. In the reaction with the mixture of H_2S, HDS, and

https://doi.org/10.1021/acsomega.2c03594
ACS Omega 2022, 7, 29337−29343

Table 1. Observed and Calculated Vibrational Frequencies (cm^{-1}) at B3LYP for HCrSH and $HCr(SH)_2$[a]

B3LYP	obsd	B3LYP	obsd	description
HCrSH		DCrSD		
2649.2(1)		1901.9(0)		S−H str
1708.2(224)	1661.8	1220.2(118)	1198.8	Cr−H str
498.5(4)		348.1(12)		H−S−Cr bend
405.7(154)		394.4(49)		Cr−S str
351.8(13)		269.8(44)		H−Cr−S bend
275.3(58)		198.1(32)		HCrSH def
$HCr(SH)_2$		$DCr(SD)_2$		
2642.4(0)		1897.1(0)		S−H str
2641.8(3)		1896.6(2)		S−H str
1740.1(110)	1683.4	1243.5(58)	1214.3	Cr−H str
565.3(13)		492.0(53)		Cr−H bend
520.4(1)		391.7(4)		S−H bend
509.0(14)		371.5(8)		S−H bend
394.9(57)		338.4(2)		Cr−S str
356.7(6)		321.6(19)		Cr−S str
255.6(11)		185.2(5)		S−H bend
250.4(19)		181.1(11)		S−H bend
102.7(60)		79.2(35)		Cr−H bend
90.7(0)		88.7(0)		S−Cr−S bend

[a]Calculated intensities (km/mol) are given in parentheses.

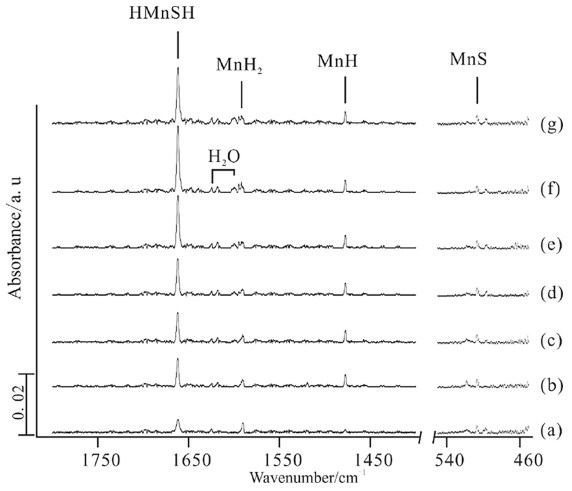

Figure 3. Spectra in selected regions from the reaction of Mn with 0.3% H_2S in the argon matrix: (a) 1 h co-deposition, (b) 25 K annealing, (c) 5 min >350 nm photolysis, (d) 5 min >300 nm photolysis, (e) 5 min >270 nm photolysis, (f) 5 min full-arc mercury lamp irradiation, and (g) 30 K annealing.

D_2S as reagents (Figure 4), the deuterium counterpart of 1661.6 cm^{-1} appeared at 1195.7 cm^{-1}, defying the H/D isotopic ratio of 1.3896. The 1661.6 cm^{-1} absorption is slightly lower than the Mn−H stretching mode of HMnOH (1663.4 cm^{-1}).[20] The band position and H/D isotopic ratio are suitable for the Mn(II)−H stretching vibration, and this absorption is assigned to the Mn−H stretching mode of HMnSH.

DFT calculations predict HMnSH to have a C_s symmetric structure at the $^6A'$ ground state. The Mn−H stretching vibration predicted at 1695.0 cm^{-1} overestimates the experimental value by 2.0% (Table 2). The predicted H/D isotopic ratio (1.4015) is in good agreement with the experimental value of 1.3896.

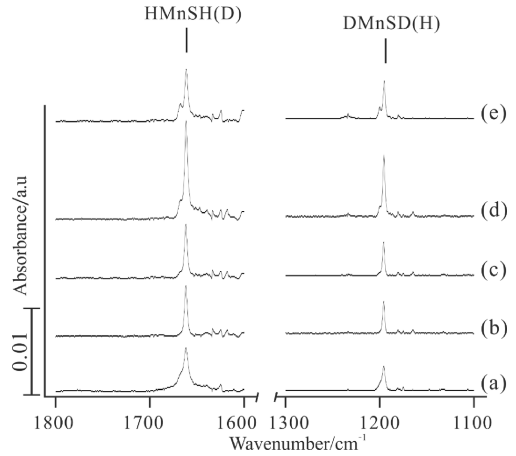

Figure 4. Spectra in selected regions from the reaction of Mn with 0.1% H_2S + 0.1% HDS + 0.1% D_2S in the argon matrix: (a) 1 h co-deposition, (b) 25 K annealing, (c) 5 min >400 nm photolysis, (d) 5 min >270 nm photolysis, and (e) 5 min full-arc mercury lamp irradiation.

Table 2. Observed and Calculated Vibrational Frequencies (cm^{-1}) at B3LYP for HMnSH[a]

B3LYP	obsd	B3LYP	obsd	description
HMnSH		DMnSD		
2655.9(2)		1906.6(1)		S−H str
1695.0(325)	1661.6	1209.4(175)	1195.7	Mn−H str
493.3(9)		337.2(8)		H−S−Mn bend
367.2(39)		385.4(38)		Mn−S str
230.9(143)		168.7(79)		H−Mn−S bend
205.2(160)		149.3(86)		HMnSH def

[a]Calculated intensities (km/mol) are given in parentheses.

HFeSH and $HFeSHSH_2$. In the reaction of laser-ablated Fe atoms with H_2S in solid argon (Figure 5), absorption at 1731.6 cm^{-1} appeared as weak absorption after co-deposition and doubled on annealing to 25 K. The absorption negligibly changed on >400 nm photolysis but sharply increased (by over 500%) on >350 nm photolysis. Upon full-arc mercury lamp

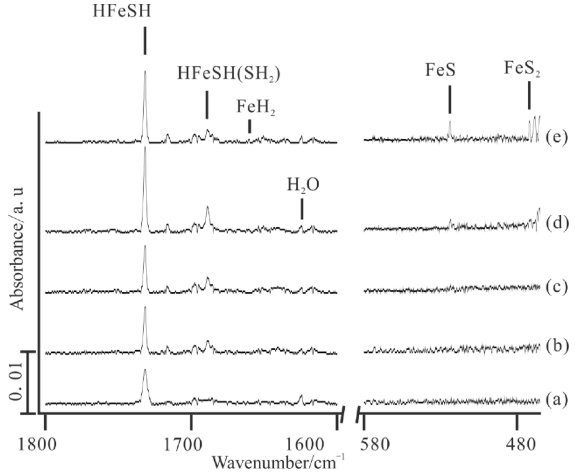

Figure 5. Spectra in selected regions from the reaction of Fe with 0.3% H_2S in the argon matrix: (a) 1 h co-deposition, (b) 25 K annealing, (c) 5 min >350 nm photolysis, (d) 5 min >270 nm photolysis, and (e) 5 min full-arc mercury lamp irradiation.

https://doi.org/10.1021/acsomega.2c03594
ACS Omega 2022, 7, 29337−29343

irradiation (>220 nm), the 1731.6 cm^{-1} absorption decreased by about 10% along with the enhancement of absorptions due to FeS (523.2 cm^{-1}) and FeS_2 (471.1 cm^{-1}).[16] It suggests that the composite contributing to the 1731.6 cm^{-1} absorption converts to FeS upon full-arc mercury lamp irradiation. The 1731.6 cm^{-1} absorption shifts to 1246.2 cm^{-1} in the reaction with D_2S as a reagent (Figure 6), giving an H/D isotopic ratio

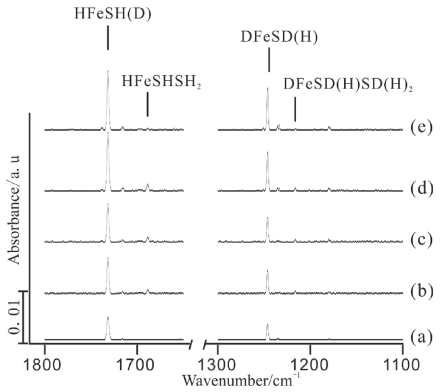

Figure 6. Spectra in selected regions from the reaction of Fe with 0.1% H_2S + 0.1% HDS + 0.1% D_2S in the argon matrix: (a) 1 h co-deposition, (b) 25 K annealing, (c) 5 min >400 nm photolysis, (d) 5 min >270 nm photolysis, and (e) 5 min full-arc mercury lamp irradiation.

of 1.3895. Compared with the Fe−H stretching vibration of HFeOH[17] (1731.9 cm^{-1}), FeH_2 (1694 cm^{-1}), and FeH_3 (1646.1 cm^{-1})[15] in the solid argon matrix, the 1731.6 cm^{-1} absorption is suitable for the Fe(II)−H stretching vibration. Accordingly, this absorption is assigned to HFeSH.

Absorption at 1688.9 cm^{-1} increased upon >270 nm photolysis. In the experiments with D_2S as the reagent, the absorption shifts to 1216.3 cm^{-1}, defying the H/D isotopic ratio of 1.3886. This absorption lies close to the Fe−H stretching vibration of HFeSH. The band position and H/D isotopic ratio are appropriate to the Fe(II)−H stretching vibration. The 1688.9 cm^{-1} absorption showed the same behaviors as the 1731.6 cm^{-1} absorption in the annealing and photochemical processes. This absorption is suitable for the Fe−H stretching vibration of $HFeSHSH_2$.

HFeSH is predicted to have a C_s symmetric structure at the $^5A'$ ground state by DFT calculations. The Fe−H stretching vibration of HFeSH predicted at 1757.7 cm^{-1} is in good consistency with the experimental value of 1731.6 cm^{-1} (Table 3). The predicted H/D isotopic ratio of 1.4012 is also in good agreement with the experimental value of 1.3895. The Fe−H stretching vibration of $HFeSHSH_2$ predicted at 1718.4 cm^{-1} overestimates the experimental value (1688.9 cm^{-1}) by 1.7%. Theoretical calculations give additional evidence for our assignments.

DISCUSSION

The reactions of laser-ablated transition metal atoms M (M = Cr, Mn, and Fe) with hydrogen sulfide in the low-temperature argon matrix were conducted, and the products were identified by infrared spectroscopy. Figures 7 and 8 present the optimized structures of relative species and energy profiles along the reaction coordinate from M + H_2S to HMSH. The insertion of one M atom into one S−H bond of H_2S is thermodynamically driven. The reaction of ground-state

Table 3. Observed and Calculated Vibrational Frequencies (cm^{-1}) at B3LYP for HFeSH and $HFeSHSH_2$[a]

B3LYP	obsd	B3LYP	obsd	description
HFeSH		DFeSD		
2648.8(2)		1901.8(1)		S−H str
1757.7(322)	1731.6	1253.8(173)	1246.2	Fe−H str
615.3(14)		452.3(10)		HFeSH def
401.0(89)		287.3(44)		H−S−Fe bend
381.3(36)		378.2(36)		Fe−S str
69.1(159)		50.8(87)		H−Fe−S bend
$HFeSHSH_2$		$DFeSDSD_2$		
2686.1(7)		1927.3(3)		S−H str
2671.6(6)		1918.4(0)		S−H str
2667.9(1)		1915.3(2)		S−H str
1718.4(347)	1688.9	1232.1(187)	1216.3	Cr−H str
1205.0(1)		863.2(0)		SH_2 bend
508.5(3)		382.2(27)		H−S−Fe bend
437.9(17)		353.3(28)		SH_2 bend
396.3(14)		308.3(4)		SH_2 bend
360.8(42)		287.9(14)		Fe−S str
302.5(113)		215.9(42)		HFeSH def
223.8(126)		170.6(21)		S−Fe−H bend
164.7(10)		149.9(54)		Fe−S str
125.0(13)		85.4(7)		HFeSH def
62.3(1)		62.7(4)		S−Fe−S bend
32.1(15)		38.2(5)		$FeSH_2$ def

[a]Calculated intensities (km/mol) are given in parentheses.

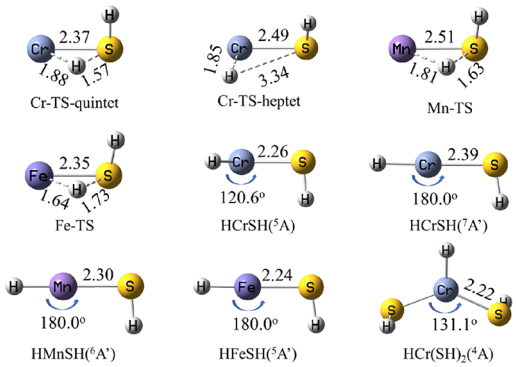

Figure 7. Optimized structures of relative species by B3LYP calculations. The bond lengths and angles are in angstroms and degrees, respectively.

Cr:$a^7S(3d^54s^1)$ with H_2S releases heat of 23.3 kcal/mol, but the reaction is hindered by a reaction barrier of 12.6 kcal/mol on the ground-state surface. In the low-temperature argon matrix, absorptions assigned to HCrSH exhibited no change but greatly increased upon >400 nm photolysis. The $z^7P \leftarrow {}^7S$ transition of Cr atoms occurred at 396 nm in a low-temperature krypton matrix.[21] The experimental results indicate that the reaction between Cr and H_2S only takes place after the excitation of chromium atoms to the Cr:$z^7P(3d^54p^1)$ excited state on >400 nm photolysis. Theoretical studies indicate that the first step for the inserting reaction is the formation of the MSH_2 complex by the approaching of transition metal atoms to H_2S molecules.[6,22] As shown in Figure 9, the interaction energy between ground-state Cr and H_2S is 1.36 kcal/mol at a Cr−S distance of 3.1 Å, which is assigned to the van der Waals force. A stable complex could be formed between excited-state Cr:$z^7P(3d^54p^1)$ atoms

https://doi.org/10.1021/acsomega.2c03594
ACS Omega 2022, 7, 29337−29343

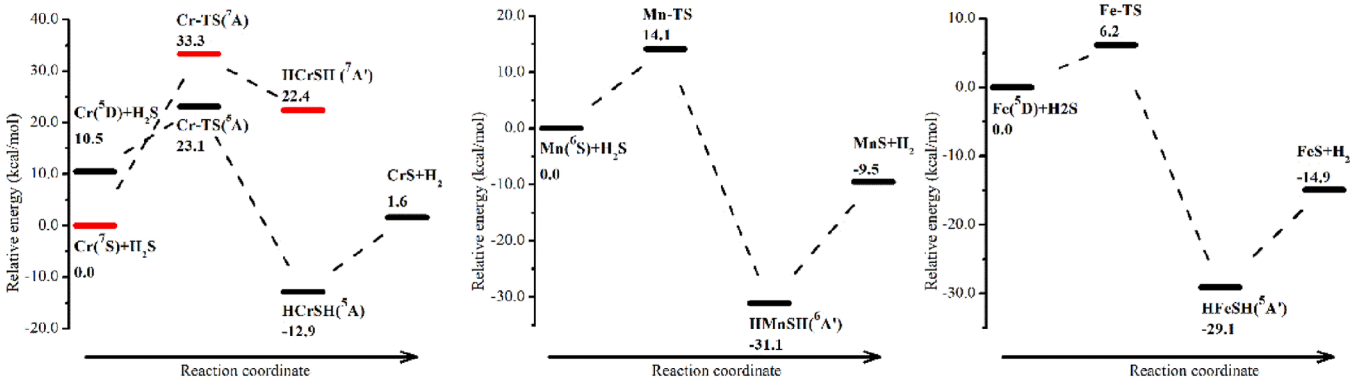

Figure 8. Potential energy profiles along the reaction coordinate from M + H_2S to HMSH (M = Cr, Mn, and Fe).

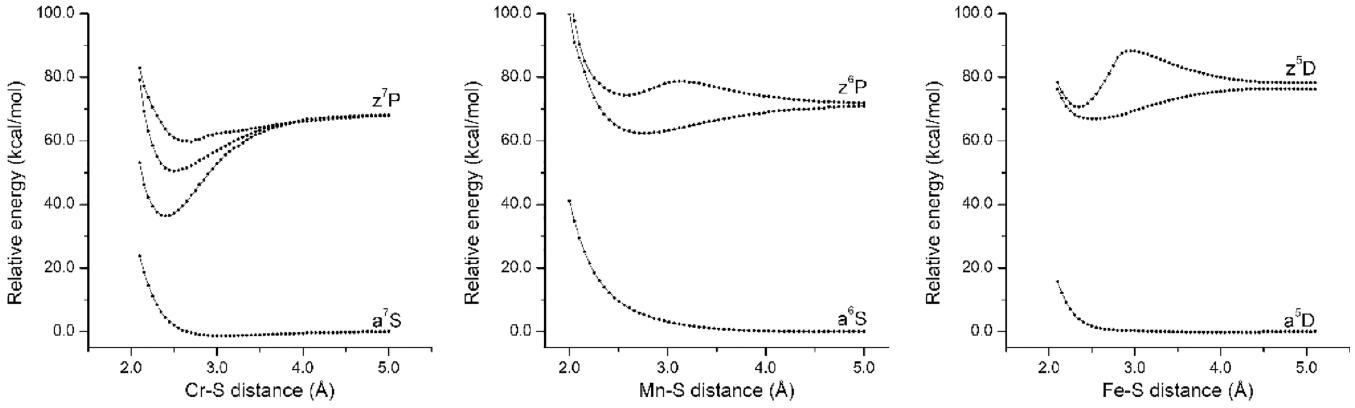

Figure 9. Potential energy curves of the interaction of M (M = Cr, Mn, and Fe) and H_2S with respect to M−S distances calculated by TDDFT at the B3LYP theoretical level.

and H_2S with a binding energy of 31.6 kcal/mol at a Cr−S bond length of 2.35 Å (Figure 9). The formed excited-state MSH_2 rearranges to HCrSH spontaneously on the heptet state surface followed by spin-forbidden surface crossing and nonradiative decay to a quintet ground state. As shown in Figure 8, the quintet ground-state HCrSH(^{5}A) is 35.3 kcal/mol lower in energy compared with heptet ground-state HCrSH(^{7}A′). The transition state linking the reactants and insertion products on the quintet state is 10.2 kcal/mol lower in energy compared with that on the heptet state surface. It suggests that the spin-forbidden surface crossing occurred before the transition state.

Reactions of Mn and Fe with H_2S are spin-conserved. As shown in Figure 9, interactions between ground-state Mn and Fe atoms and H_2S are totally repulsive. The repulsive interaction hindered the approaching of the two reactants for further reaction. The reaction barriers of 14.0 and 6.2 kcal/mol for the reactions of ground-state Mn:a^{6}S($3d^54s^2$) and Fe:a^{5}D-($3d^64s^2$) with H_2S also inhibited the occurrences of the reactions. Absorptions assigned to HMnSH start to increase on >350 nm photolysis. The a^{6}S → z^{6}P transition of manganese atoms occurred at 397.4 nm.[23] In our experiments, excited-state Mn:z^{6}P($3d^54s^14p^1$) atoms produced upon >350 nm photolysis become attractive to H_2S with a binding energy of 8.5 kcal/mol. The formed MSH_2 complex rearranges to HMnSH spontaneously followed by nonradiative decay to the ground state via conical intersection. Similarly, laser-ablated Fe atoms react with H_2S upon >350 nm photolysis in the solid argon matrix. The a^{5}D → z^{5}D transition of Fe atoms occurs at 386.0 nm in the argon matrix.[23] The interaction between Fe atoms and H_2S molecules is totally repulsive on the ground state and becomes attractive after the excitation of Fe to the Fe:z^{5}D($3d^64s^14p^1$) state on >350 nm photolysis (with a binding energy of 9.5 kcal/mol). The experimental results indicate that the reaction of ground-state transition metals M (M = Cr, Mn, and Fe) with H_2S is hindered by the repulsive interaction and the reaction barrier on the ground-state surface. In the solid argon matrix, laser-ablated group 4[5] and group 5[6] transition metal atoms react with H_2S on the annealing process. Theoretical studies indicate that stable complexes can be formed by the donation of electrons from H_2S to transition metal atoms (group 4 and group 5). The formed hot complexes rearrange to the insertion products spontaneously. Meanwhile, the activation of H_2S by group 12 metal atoms[24] and transition metal atoms studied here occurred upon photolysis. Quantum chemical calculations suggest that the interactions between H_2S molecules and ground-state transition metal atoms M (M = Zn, Cd, Hg, Cr, Mn, and Fe) are repulsive. After being excited to corresponding excited states upon photolysis, the excited-state transition metal atoms become attractive to H_2S, leading to the formation of the complex MSH_2 on the excited state. The produced hot complex [MSH_2]* can further rearrange to insertion products by surmounting the reaction barrier on the ground-state surface. Experimental and theoretical studies conclude that the formation of a stable complex by the approaching of transition metal atoms to H_2S molecules is the vital process for the activation of H_2S. H_2S can be activated by a metal atom that is attractive to a H_2S molecule to produce the stable complex MSH_2 for further reaction.

https://doi.org/10.1021/acsomega.2c03594
ACS Omega 2022, 7, 29337−29343

Upon full-arc mercury lamp irradiation, absorptions assigned to HMSH (M = Cr, Mn, and Fe) decreased along with the enhancement of absorptions due to MS. The experimental results indicate that the MS molecules are produced by the elimination of hydrogen from HMSH upon photolysis. As shown in Figure 8, the elimination of hydrogen from HMSH is endothermic. The energy needed for the splitting of hydrogen from HMSH could be supplied by photolysis. In the argon matrix, metal sulfides and hydrogen are produced by the reaction of M atoms with H_2S upon photolysis, which delivers a possible way to reproduce hydrogen from H_2S with the participation of transition metal atoms.

CONCLUSIONS

Matrix isolation infrared spectroscopy and quantum chemical calculations were employed to study the reaction of laser-ablated M (M = Cr, Mn, and Fe) atoms with hydrogen sulfide in a 5 K argon matrix. Experimental and theoretical results indicate that the activation of H_2S by M atoms takes place upon photolysis. The ground-state Mn and Fe atoms are repulsive to hydrogen sulfide molecules, and ground-state Cr atoms were slightly attractive to H_2S molecules by van der Waals force. The excited-state Cr:$z^7P(3d^54p^1)$, Mn:y^6P-$(3d^54s^14p^1)$, and Fe:$z^5D(3d^54s^14p^1)$ atoms produced on photolysis become attractive to H_2S molecules with relatively large binding energies. The activation of H_2S by Cr atoms takes place upon irradiation at longer wavelength compared with Mn and Fe. It suggests that Cr atoms are more suitable for the photochemical activation of H_2S among the three kinds of metal atoms investigated in this work. The formed MSH_2 rearranges to HMSH spontaneously. Upon full-arc mercury lamp irradiation, metal sulfides were produced by the elimination of hydrogen from HMSH molecules.

ASSOCIATED CONTENT

Supporting Information

The Supporting Information is available free of charge at https://pubs.acs.org/doi/10.1021/acsomega.2c03594.

Spectra in selected regions from the reaction of Cr atoms with H_2S (PDF)

AUTHOR INFORMATION

Corresponding Author

Xuefeng Wang − *School of Chemical Science and Engineering, Tongji University, Shanghai 200092, China;* orcid.org/0000-0001-6588-997X; Email: xfwang@tongji.edu.cn

Author

Jie Zhao − *School of Chemistry and Chemical Engineering, Guizhou University, Guiyang 550025 Guizhou, China; School of Chemical Science and Engineering, Tongji University, Shanghai 200092, China;* orcid.org/0000-0002-8463-5913

Complete contact information is available at: https://pubs.acs.org/10.1021/acsomega.2c03594

Notes

The authors declare no competing financial interest.

ACKNOWLEDGMENTS

This work is supported by the Science and Technology Fund of Guizhou Province (no. 2020-1Y046).

REFERENCES

(1) Schreiner, B. Der Claus-Prozess. Reich an Jahren und bedeutender denn je. *Chem. unserer Zeit* **2008**, *42*, 378−392.

(2) Reddy, S.; Nadgouda, S. G.; Tong, A.; Fan, L. S. Metal sulfide-based process analysis for hydrogen generation from hydrogen sulfide conversion. *Int. J. Hydrogen Energy* **2019**, *44*, 21336−21350.

(3) Guldal, N. O.; Figen, H. E.; Baykara, S. Z. Perovskite catalysts for hydrogen production from hydrogen sulfide. *Int. J. Hydrogen Energy* **2018**, *43*, 1038−1046.

(4) Kwok, K. M.; Ong, S. W. D.; Chen, L.; Zeng, H. C. Constrained Growth of MoS_2 Nanosheets within a Mesoporous Silica Shell and Its Effects on Defect Sites and Catalyst Stability for H_2S Decomposition. *ACS Catal.* **2018**, *8*, 714−724.

(5) Wang, Q.; Zhao, J.; Wang, X. Reactions of Ti, Zr, and Hf atoms with hydrogen sulfide: argon matrix infrared spectra and theoretical calculations. *J. Phys. Chem. A* **2015**, *119*, 2244−2252.

(6) Zhao, J.; Xu, B.; Yu, W. J.; Wang, X. F. Reactions of Group V Metal Atoms with Hydrogen Sulfide: Argon Matrix Infrared Spectra and Theoretical Calculations. *Chin. J. Chem. Phys.* **2016**, *29*, 10−20.

(7) Wang, X.; Andrews, L.; Thanthiriwatte, K. S.; Dixon, D. A. Infrared spectra of H_2ThS and H_2US in noble gas matrixes: enhanced H-An-S covalent bonding. *Inorg. Chem.* **2013**, *52*, 10275−10285.

(8) Zhao, J.; Ji, T.; Xiao, X.; Wang, X.; Beckers, H.; Riedel, S. Charge-Inverted Hydrogen-Bridged Bond in $HCa(\mu\text{-}H)_3E$ (E = Si, Ge, and Sn): Matrix Isolation Infrared Spectroscopic and Theoretical Studies. *Inorg. Chem.* **2020**, *59*, 14355−14366.

(9) Ji, T.; Zhu, B.; Zhao, J.; Yu, W.; Wang, X. Infrared Spectra and Theoretical Calculations of BSe_2 and BSe_2^-: The Pseudo-Jahn−Teller Effect. *J. Phys. Chem. A* **2021**, *125*, 3606−3613.

(10) Frisch, M. J. T. G. W.; Schlegel, H. B.; Scuseria, G. E.; Robb, M. A.; Cheeseman, J. R.; Scalmani, G.; Barone, V.; Mennucci, B.; Petersson, G. A.; Nakatsuji, H.; Caricato, M.; Li, X.; Hratchian, H. P.; Izmaylov, A. F.; Bloino, J.; Zheng, G.; Sonnenb, D. J.; Hada, M.; Ehara, M.; Toyota, K.; Fukuda, R.; Hasegawa, J.; Ishida, M.; Nakajima, T.; Honda, Y.; Kitao, O.; Nakai, H.; Vreven, T.; Montgomery, J. A.; Peralta, J. E.; Ogliaro, F.; Bearpark, M.; Heyd, J. J.; Brothers, E.; Kudin, K. N.; Staroverov, V. N.; Kobayashi, R.; Normand, J.; Raghavachari, K.; Rendell, A.; Burant, J. C.; Iyengar, S. S.; Tomasi, J.; Cossi, M.; Rega, N.; Millam, J. M.; Klene, M.; Knox, J. E.; Cross, J. B.; Bakken, V.; Adamo, C.; Jaramillo, J.; Gomperts, R.; Stratmann, R. E.; Yazyev, O.; Austin, A. J.; Cammi, R.; Pomelli, C.; Ochterski, J. W.; Martin, R. L.; Morokuma, K.; Zakrzewski, V. G.; Voth, G. A.; Salvador, P.; Dannenberg, J. J.; Dapprich, S.; Daniels, A. D.; Farkas, O.; Foresman, J. B.; Ortiz, J. V.; Cioslowski, J.; Fox, D. J., *Gaussian 09*, , Revision E.01Gaussian, Inc., Wallingford CT, 2009.

(11) Wang, X.; Andrews, L. Chromium Hydrides and Dihydrogen Complexes in Solid Neon, Argon, and Hydrogen: Matrix Infrared Spectra and Quantum Chemical Calculations. *J. Phys. Chem. A* **2003**, *107*, 570−578.

(12) Liang, B.; Andrews, L. Infrared Spectra and Density Functional Theory Calculations of Group 6 Transition Metal Sulfides in Solid Argon. *J. Phys. Chem. A* **2002**, *106*, 6945−6951.

(13) Wang, X.; Andrews, L. Matrix Infrared Spectra and Density Functional Theory Calculations of Manganese and Rhenium Hydrides. *J. Phys. Chem. A* **2003**, *107*, 4081−4091.

(14) DeVore, T. C., *SPECTROSCOPY OF TRANSITION METAL SPECIES IN RARE GAS MATRICES: I. VANADIUM METAL. II. SULFIDES. III. CARBONYL COMPLEXES. IV. DINITROGEN COMPLEXES. V. HOMONUCLEAR DIATOMIC COMPOUNDS*. 1975: Iowa State University.

(15) Chertihin, G. V.; Andrews, L. Infrared Spectra of FeH, FeH_2, and FeH_3 in Solid Argon. *J. Phy. Chem.* **1995**, *99*, 12131−12134.

(16) Liang, B.; Wang, X.; Andrews, L. Infrared Spectra and Density Functional Theory Calculations of Group 8 Transition Metal Sulfide Molecules. *J. Phys. Chem. A* **2009**, *113*, 5375−5384.

(17) Kauffman, J. W.; Hauge, R. H.; Margrave, J. L. Studies of reactions of atomic and diatomic chromium, manganese, iron, cobalt, nickel, copper, and zinc with molecular water at 15 K. *J. Phy. Chem.* **1985**, *89*, 3541−3547.

(18) Wang, X.; Andrews, L. Silylidyne, HSi≡MoH_3 and HSi≡WH_3, and Silyl Metal Hydride, SiH_3-CrH, Products in Silane Reactions. *J. Am. Chem. Soc.* **2008**, *130*, 6766−6773.
(19) Wang, X.; Andrews, L. Infrared Spectra, Structure, and Bonding of the GeH_3—CrH, HGe≡MoH_3, and HGe≡WH_3 Molecules in Solid Neon and Argon. *Inorg. Chem.* **2008**, *47*, 8159−8166.
(20) Zhou, M.; Zhang, L.; Shao, L.; Wang, W.; Fan, K.; Qin, Q. Reactions of Mn with H_2O and MnO with H_2. Matrix-Isolation FTIR and Quantum Chemical Studies. *J. Phys. Chem. A* **2001**, *105*, 5801−5807.
(21) Pellin, M. J.; Gruen, D. M.; Fisher, T.; Foosnaes, T. Emission, optical−optical double resonance, and excited state absorption spectroscopy of matrix isolated chromium and molybdenum atoms. *J. Chem. Phys.* **1983**, *79*, 5871−5886.
(22) Zhao, J.; Wang, Q.; Yu, W.; Huang, T.; Wang, X. M−S Multiple Bond in HMSH, H_2MS, and HMS Molecules (M = B, Al, Ga): Matrix Infrared Spectra and Theoretical Calculations. *J. Phys. Chem. A* **2018**, *122*, 8626−8635.
(23) Mann, D. M.; Broida, H. P. Ultraviolet Absorption Spectra of Transition Metal Atoms in Rare-Gas Matrices. *J. Chem. Phys.* **1971**, *55*, 84−94.
(24) Pan, Z.; Liu, X.; Zhao, J.; Wang, X. Infrared spectra of HMSH and HMMSH (M=Zn, Cd, Hg) in solid argon. *J. Mol. Spectrosc.* **2015**, *310*, 16−22.

https://doi.org/10.1021/acsomega.2c03594
ACS Omega 2022, 7, 29337−29343